

# Binary Neutron Star Merger Rates.

## Predictions from observations of dwarf galaxies and observable rates with ground-based gravitational-wave detectors.

Karen Perez Sarmiento

Fermi National Accelerator Laboratory. Macalester College

Supervisors: Alex Drlica-Wagner and Marcelle Soares-Santos

August 18, 2017

### Abstract

Binary Neutron Star (BNS) mergers are interesting events in the field of multi-messenger astronomy since they are promising sources of detectable gravitational wave signals and electromagnetic transients. I introduce a new method to calculate a conservative, lower-limit to the rate of (BNS) merger events that is proportional to the stellar mass, and is based on evidence of an r-process event in the dwarf galaxy Reticulum II. Two estimates of the stellar mass in the nearby universe were made using a Schechter Mass Function and a modified version of the 2MASS Extended Source Catalog (2MASS XSC). The BNS merger event rates were calculated to be 285.88 and 266.77  $Gpc^{-3}yr^{-1}$  from the Schechter Mass Function and the galaxy catalog mass estimates, respectively. Predictions of observed rates with LIGO were made considering that ground-based gravitational-wave detectors have preferential sensitivity dependent on right ascension and declination. The predicted observed rate for a 200 Mpc volume was estimated at  $6.30yr^{-1}$ .

## 1 Introduction

Binary Neutron Star (BNS) mergers are rare events for which we do not have direct observations. They are expected to be sources of detectable gravitational waves and electromagnetic signatures which, when coupled with each other, could yield a wealth of information about the nature of these events from different astrophysical standpoints. In the past, most of the work determining the astrophysical rates of BNS mergers has been done in studies of Short Gamma-Ray Bursts (SGRB). Nevertheless, current models for BNS mergers also predict other observable signatures, such as kilonovae and their consequent r-process nucleosynthesis events. This work presents a new method to calculate a conservative astrophysical rate of BNS merger events from evidence of r-process nucleosynthesis in the dwarf galaxy Reticulum II, and assumes the rate to be dependent on stellar mass. Estimates of the stellar mass in the nearby universe using a Schechter Mass function and a modified version of the 2MASS Extended Source Catalog (2MASS XSC) yield rates of 285.88 and 266.77  $Gpc^{-3}yr^{-1}$ , respectively. Moreover, observational selection effects of the ground-based gravitational-wave observatory LIGO impact observable rates of BNS mergers. Existing models of LIGO's preferential observability report dependency on right ascension and declination, and when taken into account, yield an observable rate of  $6.30 yr^{-1}$  for a 200 Mpc LIGO range. This paper is structured as follows: section 2 covers background knowledge on BNS merger signatures, observational evidence of one of these events in Reticulum II, and LIGO's observational selection effects. Section 3 introduces the new method to calculate a conservative rate of BNS merger events proportional to the stellar mass, and discusses its assumptions and caveats. Section 4 deals with the two methods to estimate the stellar mass in the nearby universe: the Schechter Mass Function and the modified version of 2MASS XSC. Section 5 states the results from the two stellar mass estimates, makes use of a model for LIGO's observational selection effects to calculate observable rates, and compares our independent method to SGRB rates reported in the literature. Section 6 includes concluding remarks and possible future work to improve predictions.

## 2 Background

### 2.1 Binary Neutron Star merger signatures

Binary Neutron Stars (BNS) are gravitationally bound systems of two neutron stars that merge through a process called inspiral. There are thousands of known Neutron Stars but only about 70 are found in binary systems. BNS systems emit gravitational waves as they orbit each other, which causes the orbital distance to decrease as the frequency of the emitted waveforms increases (Rasio and Shapiro 1999). Although they were considered the most promising sources of detectable gravitational waves, no detection of BNS mergers was made during the first two observing runs of LIGO.

In addition to gravitational-wave signals, the current model for electromagnetic signatures from BNS mergers predicts three types of transients (Mertzger and Berger 2012). The first one are Short Gamma Ray Bursts (SGRBs), which are short ( $< 2$ seconds), nonrepeating, intense flashes of relativistic photons (Berger 2014). Unlike Long Gamma-Ray Bursts, SGRBs have not been found in association with supernovae. Evidence of SGRB occurrence in early-type, elliptical galaxies points to old stellar population progenitors. Additionally, their short duration strongly suggests compact object coalescences (e.g. BNS mergers) as the most promising site for these events. The geometry of SGRBs is characterized by a beaming angle, and astrophysical rates for the occurrence of SGRBs need to be corrected for this. It is not clear that all SGRBs are associated with BNS mergers or that all BNS mergers are progenitors to SGRBs. Furthermore, they are relatively rare within the LIGO range (Mertzger and Berger 2012). Another electromagnetic signature of BNS mergers, directly associated with Short Gamma Ray Bursts, is the afterglow, visible at optical and radio wavelengths in timescales of days to weeks, respectively.

The third electromagnetic signature predicted from BNS mergers are kilonovae. Kilonovae are isotropic emissions triggered by the decay of radioactive elements, and are expected to be observable on timescales of about 1 day. Decompression of the merger ejecta allows the formation of heavier radioactive elements through r-process nucleosynthesis (Doctor et al. 2017), and the resulting beta decay may be detectable at optical/near-IR wavelengths (Berger 2014).

R-process nucleosynthesis, or rapid-neutron capture nucleosynthesis, consists on the capture of neutrons by nuclei in timescales shorter than the half-lifetime of the corresponding beta decay, thus resulting in neutron-rich nuclei. R-process events produce a distinct pattern for the chemical abundance of heavy elements. To this day, there are not direct detections of kilonovae but searches for r-process nucleosynthesis events have yielded at least a candidate event in the dwarf galaxy Reticulum II.

### 2.2 The Ultra-Faint Dwarf Galaxy Reticulum II

Reticulum II (Ret II) is an ultra-faint dwarf galaxy (UFD) in the local group recently discovered in the first year of the Dark Energy Survey (DES-Y1). Roederer et al. (2016b) and Ji et al. (2016) performed high-resolution spectroscopic analysis on nine Ret II members and reported their chemical abundance pattern. Seven of those stars follow the universal r-process pattern for elements above Ba and the discrepancy for lighter elements may be explained by an universal r-process pattern that does not extend to light r-process elements. There are several proposed mechanisms for the site of the r-process Ret II. A core-collapse supernova event is one of the proposed production sites for r-process. Nevertheless, the [Eu/Fe] abundances in Ret II are the highest found in any UFDs and about 1000 times higher than the typical yields of supernovae. This points out to a rare, single progenitor for the enhanced r-process element abundances found in Ret II (Ji et al. 2016a). In fact, the most promising site for the r-process enhancement in this galaxy is a kilonova resulting from a BNS merger since they are predicted to readily produce high abundances of r-process elements.

Table 1: Properties of Reticulum II.

$\alpha_{2000}$ (deg)	$\delta_{200}$ (deg)	Distance (kpc)	$\log_{10}(\tau)$	$\log_{10}(Gyr)$	Z
53.92	-54.05	32	10.08	$\pm 0.21$	0.0003

### 2.3 Observational Selection Effects of ground-based gravitational-wave observatories

Observable rates of BNS merger events through gravitational-wave signal are constrained by the sensitivity of the observatory. The Laser Interferometer Gravitational-wave Observatory (LIGO) network consists of two observatories located in Livingston, Louisiana and Hanford, Washington. As stated in Chen et al. (2017), this ground-based GW observatory does not have isotropic sensitivity over the whole sky. The location of the observatories creates more sensitive preferred regions at mid-latitudes (declination dependence) in the northern and southern hemispheres. Moreover, LIGO’s nonuniform daily and annual cycles create a sensitivity dependence on right ascension that does not average entirely with the rotation of the earth. Diurnal cycles and observation runs of a few months preserve longitudinal preferred regions. Figure 1 shows the preferred sensitivity regions for September 14th, 2015 and Figure 2 shows the preferred sensitivity regions for January 2017.

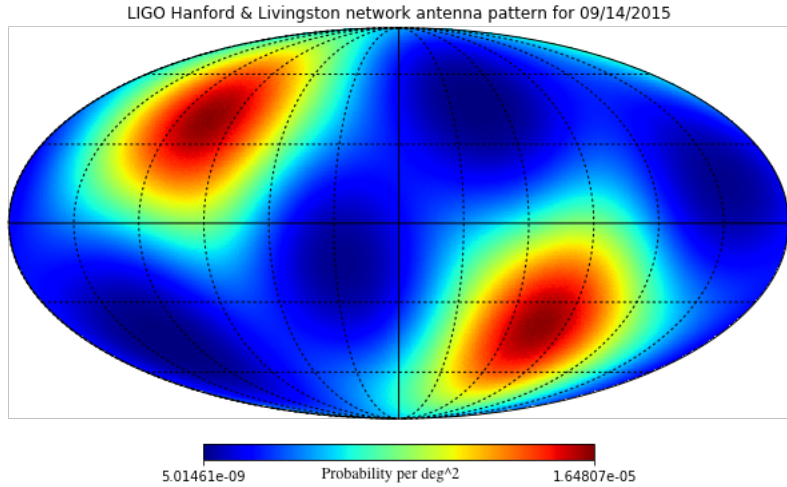


Figure 1: The LIGO Hanford and Livingston network antenna pattern in equatorial coordinates at 00:29:18 UTC on 09/14/2015. The maxima lie above North America and the Southern Indian Ocean. Figure and caption taken from Chen et al. (2017).

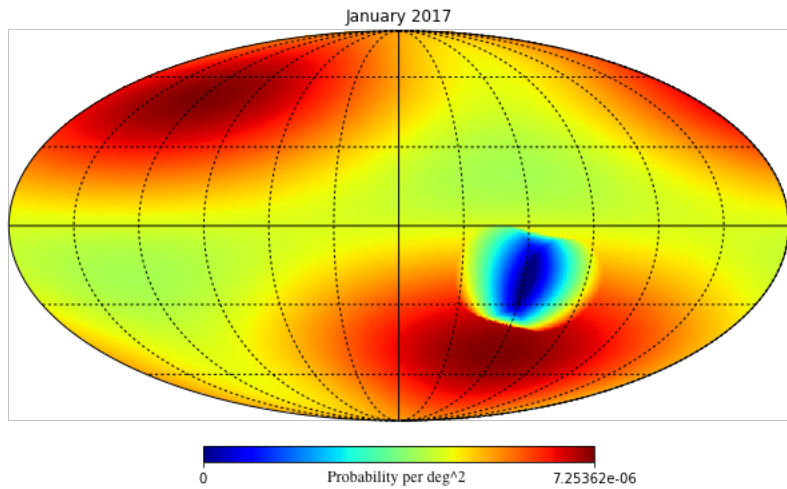


Figure 2: January 2017 preferred regions for GW detections on the celestial sphere. The Sun occludes a region  $18^\circ$  in radius (only relevant for electromagnetic follow up). Figure and caption taken from Chen et al. (2017).

### 3 Calculation of a conservative, lower limit to the rate of BNS mergers

The r-process enhancement present in Ret II, and the evidence for a rare, prolific, single event as its progenitor, strongly suggests that a BNS merger occurred in this galaxy. High-resolution spectroscopic analyses performed in another 12 dwarf galaxies show very low abundances of neutron-capture elements and therefore no evidence of prolific r-process events (Ji et al. 2016a). In this context, the candidate BNS merger event in Reticulum II can be used as the basis to calculate a conservative lower estimate to the rate of these events.

From the composite stellar mass of these 13 dwarf galaxies and by placing an upper limit to the timescale of the r-process event in Ret II, we built a simple rate calculation of BNS mergers that is assumed to scale up with stellar mass. The formula is as follows:

$$R_{BNS} = \frac{1event}{\sum_i^{13} M_* \times (T_{universe} - T_{event})} = 10^{-15} M_{\odot}^{-1} yr^{-1} \quad (1)$$

The motivation for using the stellar mass of the galaxies as the characteristic property for the rate of BNS merger events arises from the fact that it is the simplest property associated with the number of neutron stars formed within a galaxy. There is no reason to believe Ret II conforms a particular environment that enhances the existence of BNS systems and the occurrence of mergers. The fact that there is no evidence of r-process enhancement events in any of the other UFDs with known metal abundances places Ret II more on the exception than the norm. Therefore, the safest assumption is that the rate of BNS mergers scales up with galactic stellar mass. Moreover, stellar mass can easily be derived from direct observable properties, such as absolute magnitude. A BNS rate that solely depends on the stellar mass is an oversimplification. Some of the caveats of this assumption include the fact that initial mass functions are not the same for all the galaxies, nor are star formation rates in different types of galaxies. The upper limit to the timescale of the r-process event was set to the age of the universe minus the stellar population age of Ret II, which was calculated by fitting an isochrone to the color distribution of the stars ( $\tau = 13.5Gyr$ ) (Bechtol et al. 2015).

The method proposed in this work is independent on any assumptions of SGRBs, which are the typical signatures employed in the literature to estimate rates of BNS mergers. SGRBs are associated with a beaming angle, for which observable rates require correction factors that account for the number of unobserved events (Coward et al. 2012; Fong et al. 2015; Chen and Holz 2012). Moreover, it is not established whether the sole progenitors of SGRBs are BNS mergers or if all BNS mergers result in SGRBs signatures. In this sense, agreement between BNS merger rates calculated with different methods and beam-corrected SGRB rates could provide stronger evidence for the current model of the electromagnetic signatures of BNS mergers.

Table 2 states the stellar masses of the 13 Dwarf galaxies considered in the BNS merger rate calculation above.

Table 2: List of the 13 Dwarf Galaxies with High-resolution spectroscopic analysis and their stellar masses.

Name	$M_* [10^3 M_{\odot}]$	Source
Ret II	2.6	Bechtol et al. (2015)
Hor I	2.4	Bechtol et al. (2015)
Tuc II	3	Bechtol et al. (2015)
Tuc III	0.8	Drlica-Wagner et al. (2016)
Boo I	29	McConnachie (2012)
Boo II	1	McConnachie (2012)
ComBer	3.7	McConnachie (2012)
CVnII	7.9	McConnachie (2012)
Her	37	McConnachie (2012)
Segue 1	0.34	McConnachie (2012)
Segue 2	0.86	McConnachie (2012)
UMa II	4	McConnachie (2012)
Leo IV	19	McConnachie (2012)

## 4 Estimations of Stellar Mass in the nearby universe

From the previous formalism that assumes the rate of BNS mergers to be proportional to galactic stellar mass, we can obtain astrophysical rates for these events within the observable range of LIGO by estimating the stellar mass contained in a given volume. Two methods were employed for such estimation: a variation of the Schechter Mass Function integrated over a range of galactic stellar masses, and a modified version of the 2MASS XSC (complete to  $J < 15$ ) that covers the whole sky and includes properties such as the JHK magnitudes and distances for each object. Results from both methods can then be compared with each other to ensure reliability of the stellar mass estimates.

### 4.1 Schechter Mass Function approach

The Schechter Mass Function is an analytic approximation of the space density of galaxies as a function of their stellar mass (Schechter 1976). It was first derived as a luminosity function and exhibits the behavior of a power law. The formula is as follows:

$$\phi(M) = b \times \phi^* \ln(10) [10^{b(M-M^*)}]^{(1+\alpha)} \exp[-10^{b(M-M^*)}] \quad (2)$$

In this function,  $b = 1$  for the mass function,  $M^*$  is the characteristic mass in log units and determines where the mass function changes slope, and  $M$  is the mass in log units.  $\phi^*$  is the normalization and  $\alpha$  determines the slope for fainter galaxies. Values for the parameters as a function of redshift were derived by Conselice et al. (2016). They were calculated by fitting the Schechter function to galaxy surveys and catalogs at different redshifts for a standard cosmology of  $H_0 = 70 \text{ km s}^{-1}$ , and  $\Omega_m = 1 - \Omega_\lambda = 0.3$ . For the purposes of this paper, we used the parameters for the lowest redshift bin available ( $0.2 < z < 0.4$ ):  $\alpha = -1.19$ ;  $\log M^* = 11.20 M_\odot$ ;  $\phi = 22.4 \times 10^{-4} \text{ Mpc}^{-3}$ . One of the caveats of this formalism is the fact that we do not know the exact lower limit for which the function remains valid. Conselice et al. (2016) recommended a fiducial  $M_* > 10^6 M_\odot$  lower limit, since that is the typical lower limit for dwarf galaxies in the nearby universe. The function as stated calculates the number of galaxies of a given mass in a  $1 \text{ Mpc}^3$  volume. We can calculate the stellar mass from the space density of galaxies by multiplying the Schechter Mass Function by  $10^M$  and integrating over the ranges  $10^6 M_\odot$  to  $10^{12} M_\odot$ . The limits of integration were chosen from the fiducial lower mass limit of the formula and the typical sizes for the largest galaxies. The estimated stellar mass in  $1 \text{ Gpc}^3$  volume from the Schechter formalism, yields a stellar mass of  $4.09 \times 10^{17} M_\odot$ .

### 4.2 The Galaxy Catalog approach

The 2MASS Extended Source Catalog reports right ascension, declination, J, H, and K apparent magnitudes. It was complemented with distance values, calculated from photometric and spectroscopy redshifts as well as distance moduli values from several other galaxy catalogs since no single catalog was able to populate the entire distance column. Distances from distance moduli took preference, followed by spectroscopic redshifts, and finally photometric redshifts. We adopted a standard cosmology of  $H_0 = 70 \text{ km s}^{-1}$  and  $\Omega_m = 0.3$ . Below is a summary of the process followed to populate the distance column and the specific galaxy catalogs used in each step:

- a) The highest preference was given to distances calculated from distance moduli values stated in the EDD/Cosmicflows2 catalog.
- b) Second degree of preference was given to distances calculated from the distance moduli values in NED catalog.
- c) Next, distances calculated from SDSS spectroscopic redshifts were considered.
- d) NEDZ spectroscopic redshifts took the following degree of preference.
- e) Finally, for the remaining objects without distance values, distances from the 2MPZ photometric redshifts were considered.

Of the 1646844 objects in the original version of the 2MASS XSC, a total of 612837 were matched to at least one distance proxy. Table 3 shows the number and percentage of distances values that were calculated from distance moduli, spectroscopic, and photometric redshifts. Percentages were calculated from the total number of objects with at least one distance match.

Masses for each object were calculated using a mass-to-light ratio relation with J-K color (Westmeier et al. 2011; Bell and de Jong, 2001).

$$\log \frac{M/M_\odot}{L_K/L_{\odot,K}} = 1.434(J - K) - 1.380 \quad (3)$$

$$\frac{M}{M_{\odot}} = 10^{1.434(J-K) - 1.380 + 0.4(M_{\odot,K} - M_K)} \quad (4)$$

Where the absolute magnitude of the sun in K-band is  $M_{\odot,K} = 3.28$ , and  $M_K$  is the absolute magnitude of the object also in K-band.

Table 3: Distance column composition of modified version of 2MASS XSC.

Type	Number of sources	Percentage
Distance Moduli	11778	1.92
Spectroscopic redshifts	287013	46.83
Photometric redshifts	314046	51.24

The following plot shows the integrated stellar mass per pixel of the modified version of the 2MASS XSC up to a distance of 200 Mpc.

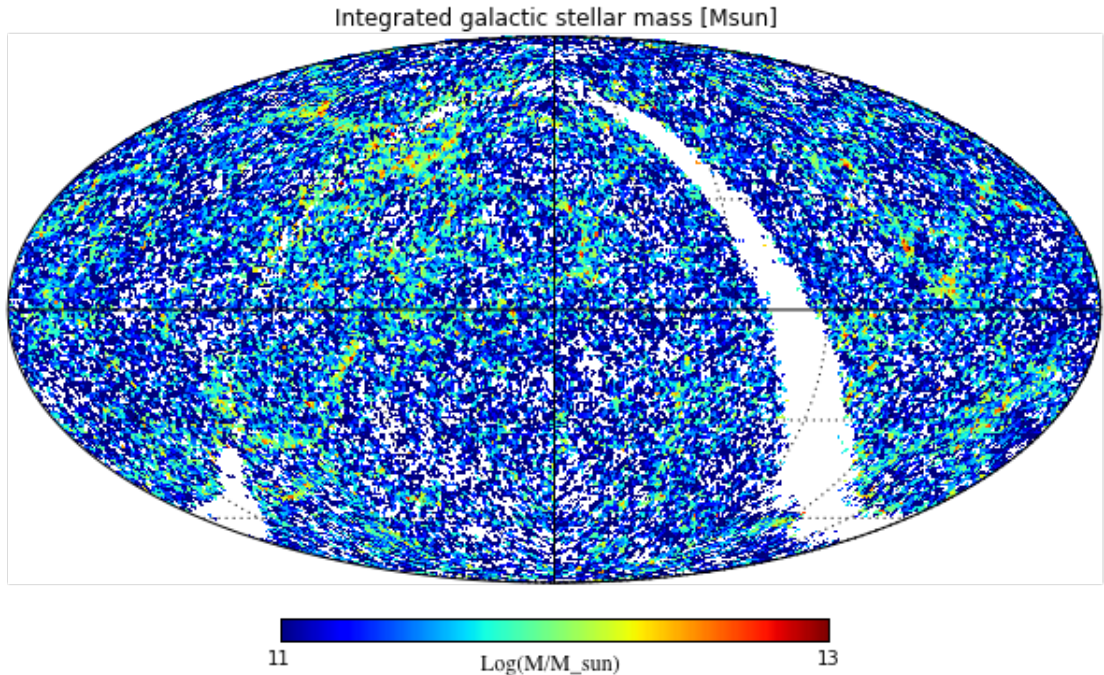


Figure 3: Integrated stellar mass [ $M_{\odot}$ ] per pixel as calculated from equation 4 for a radius of 200 Mpc. Stellar masses of objects  $M_* > 5 * 10^{12}$  were removed from catalog.

From figure 3, it is possible to match the overdense regions in the map with known galaxy clusters, i.e. the Coma Cluster and the Virgo Supercluster.

## 5 Results

Figure 4 shows the integrated BNS merger rates per pixel up to a distance of 200 Mpc as calculated from the integrated stellar masses per pixel from figure 3.

The total integrated stellar mass for a 200 Mpc volume as estimated by the galaxy catalog is  $1.28 \times 10^{16} M_{\odot}$ . We integrated the stellar mass in distance bins from 0 to 200 Mpc in increments of 20 Mpc, in order to calculate rates at those specific distances. BNS merger rates were also calculated from the Schechter formalism by scaling up the estimated stellar mass in  $1 Mpc^3$  for radii ranging from 0 to 200 Mpc.

In order to predict the number of observable BNS merger events with LIGO, the observational selection effects of the GW observatory discussed in the introduction must be taken into account. We used monthly maps of LIGO's sensitivity pattern taken from Chen et al. (2017), and multiplied them



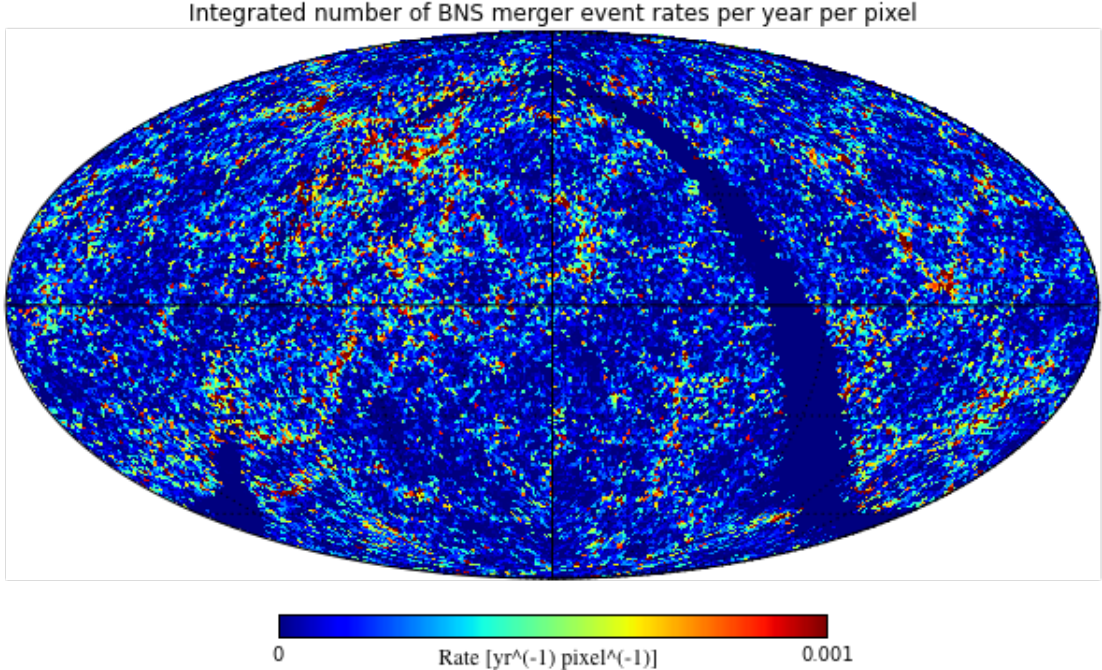


Figure 4: Integrated BNS merger rates per pixel up to a distance of 200 Mpc as calculated from equation 1 and the integrated stellar mass map in figure 1.

by the integrated BNS merger rate map created with the galaxy catalog to obtain individual monthly and composite year predictions for the number of observable events with LIGO. We assumed LIGO’s sensitivity to be independent from distance, which is not the case. Nevertheless, future LIGO upgrades are in place to push its sensitivity up to 200 Mpc. By using this method, we calculated an observable BNS merger rate of  $6.3 \text{ yr}^{-1}$  for a 200 Mpc radius.

Moreover, we performed a literature search of SGRBs beam-corrected rates. Fong et al. (2015) predicted a beam-corrected rate of  $R_{true} = 270_{-180}^{+1580} \text{ Gpc}^{-3} \text{ yr}^{-1}$  from analysis of broadband afterglow and opening angle measurements of a SGRB catalog. Coward et al. (2012) also predicted both a SGRB lower rate density of  $R_{lower} = 8_{-3}^{+5} \text{ Gpc}^{-3} \text{ yr}^{-1}$  and a beaming corrected upper limit of  $R_{upper} = 1100_{-470}^{+700} \text{ Gpc}^{-3} \text{ yr}^{-1}$ , accounting for the dominant bias in the sample of SGRBs with reasonably firm redshifts. Figure 5 shows the BNS merger rates calculated with the Schechter formalism approach, the galaxy catalog approach, and the observable rate considering LIGO’s nonuniform sensitivity. These rates are compared to SGRB rates reported in Fong et al. (2015) and Coward et al. (2012).

From the plot we can see that there is very good agreement between the rates calculated with the Schechter Function and the rates from the Galaxy Catalog for nearly every distance. This gives us confidence in the two independent methods we used to estimate the stellar mass in the nearby universe.

Moreover, it is important to notice that our BNS merger rates are within the range of lower limits proposed by Coward et al. (2012) and Fong et. al (2015). The general agreement between SGRB literature rates and the BNS merger rates calculated through our independent method based on the r-process event in Ret II points to the close relation between BNS merger rates and SGRBs beyond theoretical models.

## 6 Conclusion

The method to calculate BNS merger events based on evidence of an r-process event in Reticulum II that scales up with stellar mass yields rates comparable to beam-corrected lower limits to rates of SGRBs in the literature. The two approaches used in this work to estimate the stellar mass in the nearby universe yield very similar results:  $285.88$  and  $266.77 \text{ Gpc}^{-3} \text{ yr}^{-1}$  for the Schechter Mass Function and the galaxy catalog approach, respectively. For a 200 Mpc volume, we would expect BNS merger rates of

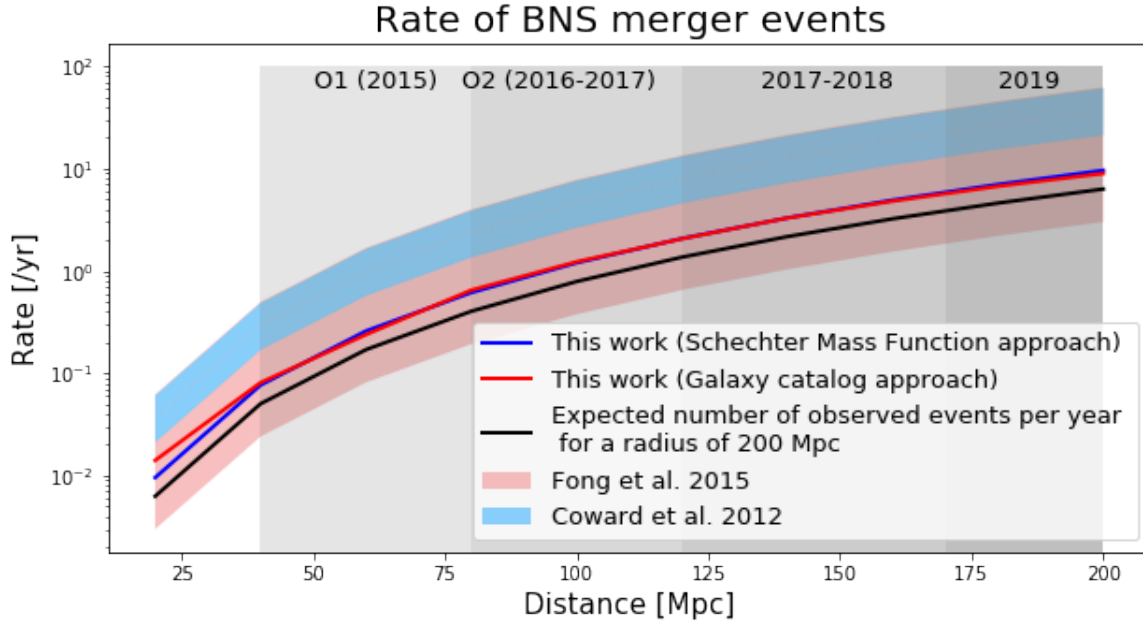


Figure 5: BNS merger rates for different radial distances calculated based on two independent estimates of the stellar mass in the nearby universe, and observable rates with LIGO, as compared to SGRBs rates reported in the literature. Rates are shown for the scales of LIGO’s range in past, present, and upcoming observing runs.

$9.58 \text{ yr}^{-1}$  according to the Schechter formalism and  $8.93 \text{ yr}^{-1}$  from the galaxy catalog estimate. When the nonuniform sensitivity of LIGO for certain of the sky is taken into account, the predicted observable rate in a 200 Mpc volume is  $6.3 \text{ yr}^{-1}$ .

Future work must be done on using distance-dependent LIGO sensitivity maps to come up with better predictions on observable rates. Moreover, a lower limit to the timescale of BNS mergers should be estimated to further constraint BNS rates. Different methods to calculate the rate of BNS mergers from the event in Ret II could take into account Star Formation Histories and Star Formation Rates to avoid the oversimplification of stellar mass dependent rates.

## References

- Annis, J., et al. Private communication (2015).  
 Bechtol, K., et al. ApJ 807, no. 1 (2015): 50.  
 Bell E. F. and de Jong R. S. AJ 550, no. 1 (2001): 212.  
 Berger, E. Annu. Rev. Astron. Astrophys. 52, no. 1 (August 18, 2014): 43–105.  
 Chen, H. Y., et al. ApJ 835, no. 1 (2017): 31.  
 Chen, H. Y. and Holz D. E. Phys. Rev. Lett. 111, no. 18 (October 31, 2013): 181101.  
 Conselice, C. J., et al. ApJ 830, no. 2 (2016): 83.  
 Coward, D. M., et al. MNRAS 425, no. 4 (October 1, 2012): 2668–73.  
 Drlica-Wagner A., et al. ApJ 813, no. 2 (2015): 109.  
 Fong, W., et al. Ap J 815, no. 2 (2015): 102.  
 Ji, A. P., et al. Nature 531, no. 7596 (March 31, 2016): 610–13.  
 Ji, A. P., et al. ApJ 830, no. 2 (2016): 93.  
 McConnachie A. W. AJ 144, no. 1 (2012): 4.  
 Metzger B. D. and Berger E. ApJ 746, no. 1 (2012): 48.  
 Rasio, F. A. and Shapiro, S. L., “Coalescing Binary Neutron Stars.” Classical and Quantum Gravity 16, no. 6 (1999): R1.  
 Roederer I. U., et al. AJ 151, no. 3 (2016): 82.  
 Westmeier, T., R. Braun, and B. S. Koribalski. MNRAS 410, no. 4 (February 1, 2011): 2217–36.